

# Studying effect of carrier fluid viscosity in magnetite based ferrofluids using optical tweezers

S Savitha<sup>1#</sup>, Shruthi S Iyengar<sup>1</sup>, Sharath Ananthamurthy<sup>1</sup> and Sarbari Bhattacharya<sup>1\*</sup>

<sup>1</sup> Department of Physics, Bangalore University, Bangalore, Karnataka, INDIA.

<sup>#</sup> Department of Physics, Government First Grade College, Chickballapura, Karnataka, INDIA.

\*E-mail: sarbari.bhattacharya@bub.ernet.in

**Abstract:** Ferrofluids with varying viscosities of carrier fluids have been prepared with magnetite ( $\text{Fe}_3\text{O}_4$ ) nanoparticles. The nanoparticles were synthesized by chemical co-precipitation and characterized using X-Ray Diffraction (XRD) and Field Emission Scanning Electron Microscopy (FESEM). They were found to be nearly spherical in shape with an almost uniform size of 13nm. The superparamagnetic nature of the water based ferrofluids at room temperature was established by SQUID magnetometry. Dynamic light scattering (DLS) was carried out to establish the size of the nanoparticle clusters in the ferrofluids synthesized. The results indicate an increase in cluster size with increase in carrier fluid viscosity. This is supported by results from Raman Spectroscopy. A further attempt to characterise these ferrofluids was made by studying the behaviour of well characterised non-magnetic micron sized probes that are optically trapped while suspended in the ferrofluid. An increase in carrier fluid viscosity results in a decrease in corner frequency when only the carrier fluid is used as the suspending medium. When the magnetic component is also present the corner frequency is higher than with just the carrier fluid. This relative increase happens at all laser powers at the trapping plane. This trend is also found to be independent of the size and material of the probe particle. Comparisons of various parameters that influence optical trapping lead us to believe that the enhancement could be due to a directed motion of the magnetic clusters in the presence of an optical trap.

## 1. Introduction

Ferrofluids are magnetic fluids that exhibit normal fluid like behaviour with superparamagnetic properties. Ferrofluids are basically suspensions of magnetic nanoparticles in a suitable carrier liquid. The magnetic nanoparticles are coated with suitable surfactants to prevent agglomeration. The nanoparticles involved are superparamagnetic in nature possessing a single magnetic domain and exhibit negligible retentivity and coercivity. The viscosity of ferrofluids is greatly influenced by external magnetic fields. These unusual properties of ferrofluids make them potential candidates for various industrial and biomedical applications [1, 2].

The magnetite ( $\text{Fe}_3\text{O}_4$ ) nanoparticles used in the study presented here were synthesized by co-precipitation method [3]. The ferrofluids were prepared by dispersing the as prepared magnetite in pure water and water-glycerol mixtures of varying component fractions, which yielded carrier fluids of varying viscosities, along with the use of a suitable surfactant. An increase in the viscosity of the carrier fluid is proposed to be a way of improving the stability of a ferrofluid [4].

A study on the effect of viscosity of the water glycerol carrier fluids on the stability of the magnetite based ferrofluids has been carried out and the results have been reported elsewhere [4]. Here we report on the effect of carrier fluid viscosity on the size of the magnetic nanoparticle clusters



by using the methods of DLS and Raman Spectroscopy. Further we report on the effect of increase of carrier fluid viscosity on the dynamics of an optically trapped non-magnetic micron sized probe suspended in the ferrofluid. The results suggest that this experimental technique could help further characterize a ferrofluid in terms of size of nanoparticle clusters and their behaviour in the presence of an optical trap.

## 2. Experimental Details

### 2.1 Materials:

Materials used for synthesis of ferrofluid are  $\text{FeCl}_3 \cdot 6\text{H}_2\text{O}$ ,  $\text{FeSO}_4 \cdot 7\text{H}_2\text{O}$ , NaOH, HCl, Tetra Methyl Ammonium Hydroxide (TMAOH), pure water and glycerol. Reagent grade materials were used without further purification. Double Distilled water was used as a solvent.

### 2.2 Methods:

**2.2.1 Synthesis of Magnetite.** The method of synthesis followed for  $\text{Fe}_3\text{O}_4$  nanoparticles is as described in [3]. The prepared powder is mixed with distilled water which is then decanted out with the aid of a strong magnet to avoid loss of the magnetic component. This process is repeated till pH is between 9 and 10. The wet precipitate is then dried in a furnace at  $150^\circ\text{C}$  for 3hrs. The resulting powder is used for XRD and FESEM characterization.

**2.2.2 Synthesis of Ferrofluid.** Magnetite powder is soaked overnight in 1M NaOH solution and then dried in an oven at  $70^\circ\text{C}$  for 2hrs. The powder is washed with hot water several times to remove Na particles on the surface [5]. The wet particles are then dispersed in pure water and water-glycerol (30, 50 and 70 % v/v) along with 10% volume fraction of surfactant and ultrasonicated using a bath till the nanoparticles are completely dispersed in the liquid.

### 2.3 Experimental Set up:

The Raman Spectra of the ferrofluid samples were recorded using the 732nm excitation line in a Raman spectrometer while the DLS measurements were made using laser light of wavelength 532nm and detecting the scattered light with a photomultiplier tube placed at angles  $75^\circ$ ,  $90^\circ$  and  $105^\circ$ . The magnetic properties of the ferrofluid synthesized were measured with Superconducting Quantum Interference Device (Quantum Design) magnetometer with a capacity to use magnetic fields up to 5T.

The optical tweezer is built using a single beam infrared laser (830nm, 100mW, Thorlabs, USA). The experimental set up and schematic is as shown in Figure 1 [6]. The laser beam is reflected by a set of mirrors and periscope arrangement and is made to fall on an oil immersion objective lens with a high numerical aperture (1.25 NA, Olympus). The sample is mounted on an XY stage which has high precision movement enabled through a piezoelectric transducer (PZT) and is located above the objective. The laser light gets focussed on the sample and the back scattered light is reflected and made to fall on a beam splitter (BS), which splits the light into two parts. First part is focussed on to a position sensitive quadrant cell photo receiver which in turn is connected to data acquisition panel, 16 bit DAC and is captured by a LABVIEW program. The second part is received by a scientific grade CMOS image sensor camera (EDC-3000, Electrim corporation, USA), using which the image of the trapped bead can be visualised. A filter is attached to the camera to prevent damage against infrared radiation. The entire tweezer arrangement is set up on a vibration isolation system (Holmarc, India) [7].

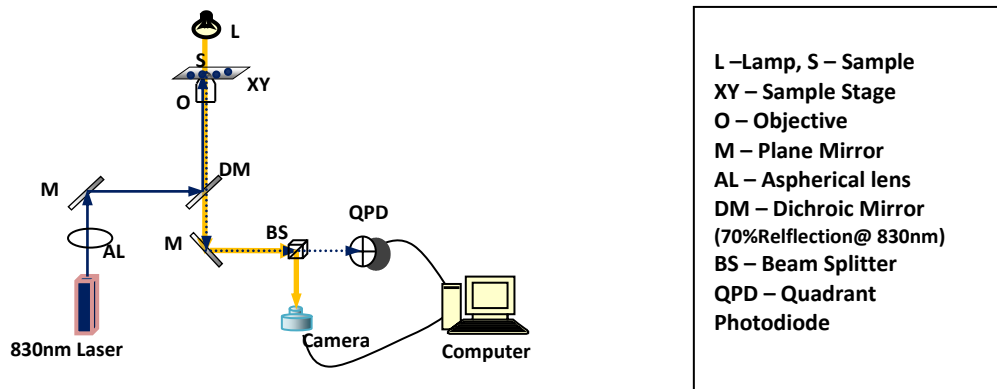


**Figure 1:** Schematic view of the optical tweezer set up. This set up is identical to the one used in [6].

### 3. Results and Discussions

#### 3.1 Structural and Morphological analysis.

Magnetite has inverse spinel structure with unit cell having fcc pattern. The prepared magnetite sample appears to be in single phase and peaks match with that of the standard pattern for Fe<sub>3</sub>O<sub>4</sub> (JCPDS 19-0629). Using the Debye Scherrer relation, given below, the mean crystalline size is calculated.

$$D = \frac{0.9\lambda}{\beta \cos\theta} \tag{1}$$

where  $\lambda$  is the wavelength of X-ray (1.5406 Å for CuK $\alpha$ ) and  $\beta$  is the full width at half maximum (FWHM) in radians [8]. The estimated size is found to be 13nm. The interplanar distance calculated for the strongest peak using the formula,

$$d = \frac{\lambda}{2 \sin\theta} \tag{2}$$

is found to be 2.519 Å. The lattice parameter ‘a’ using the value of interplanar distance,

$a = d\sqrt{h^2 + k^2 + l^2}$  is 8.35Å<sup>0</sup> which is comparable with standard lattice parameter value of 8.39Å<sup>0</sup> reported for magnetite [2]. A typical XRD pattern is as shown in Figure 2(a). FESEM image shown in Figure 2(b) reveals as prepared magnetite to be agglomerated. This is possibly because there is no surfactant used here. With the use of surfactant (TMAOH) for preparation of ferrofluids, the agglomeration effect is reduced.

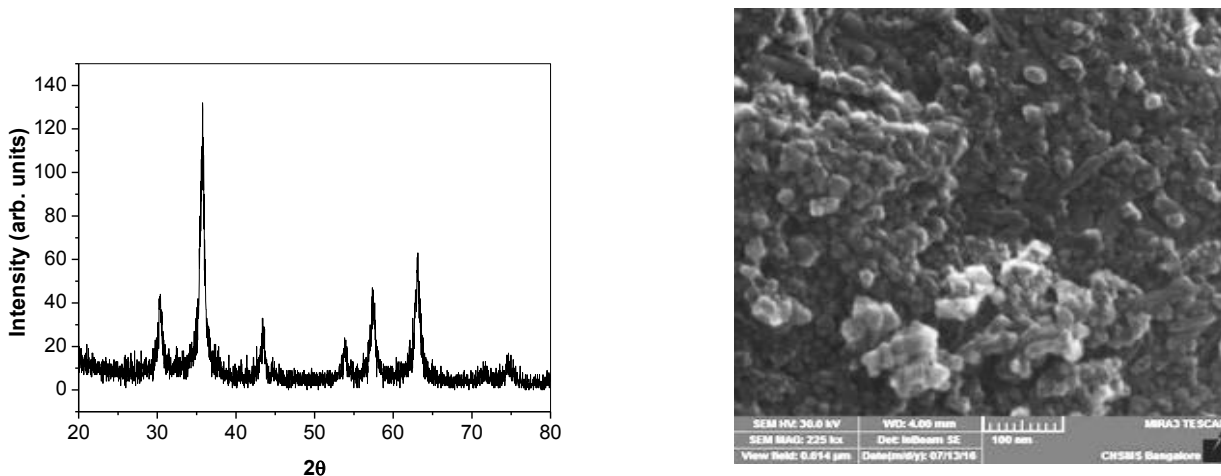


**Figure 2** (a) XRD pattern of Magnetite (b) FESEM image of as prepared magnetite (no surfactant).

### 3.2. Dynamic Light Scattering Study of ferrofluid:

DLS is based on the principle of obtaining spectral information from time dependent fluctuations of light scattered from a colloidal substance of limited volume. The normalised intensity autocorrelation response is plotted against time delay for the ferrofluid with pure water as the carrier fluid is shown in Figure 3. An exponential fit to the variation is also shown.

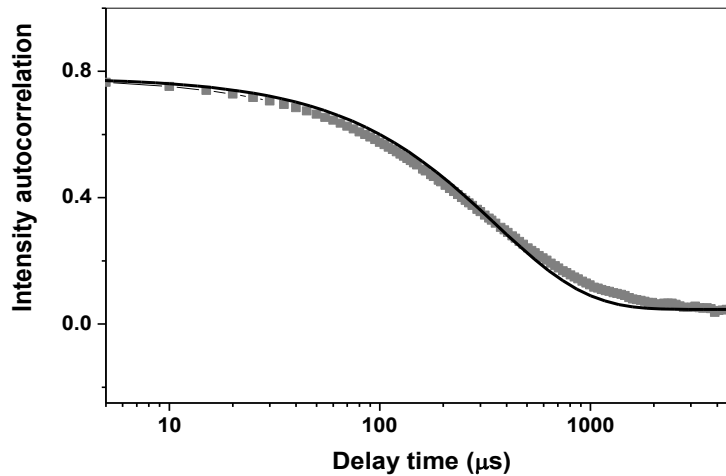


**Figure 3:** Variation of normalised intensity autocorrelation response with time delay. The continuous line gives an exponential fit for the variation.

The cluster size (hydrodynamic radius) is obtained using the Stokes-Einstein relation:

$$r_h = \frac{k_B T}{6\pi\eta D} \quad (3)$$

where 'T' is the temperature of the medium, 'D' is the diffusion co-efficient related to relaxation time ( $\tau$ ),  $k_B$  is the Boltzmann constant and ' $\eta$ ' is the viscosity of carrier liquid used [9].

$$D = \frac{1}{\tau q^2} \quad (4)$$

where 'q' is the scattered wave vector [10] which in turn depends on refractive index (n) of the carrier fluid and scattering angle ( $\theta$ ) by the relation,

$$q = \frac{4\pi n}{\lambda} \sin \frac{\theta}{2} \quad (5)$$

We find that as the viscosity of the carrier fluid is increased by increasing the volume fraction of glycerol, the cluster sizes of the magnetic nanoparticles determined by using DLS, also increases as shown in Table 1.

**Table 1:** Variation of cluster size with viscosity.

Carrier Fluid used in Ferrofluid	Cluster Size (in nm)
Pure Water	59
Water+Glycerol (50:50 v %)	266.5
Water + Glycerol (30:70 v %)	1135

**3.3 Magnetic Characterizations:**

The magnetization measurement for water based ferrofluid has been taken from -10kOe to +10kOe field. Magnetization curve at room temperature (RT) for this ferrofluid is shown in Figure 4 and does not exhibit any measurable values of coercivity or retentivity. This confirms that the synthesized samples exhibit superparamagnetism at RT [11]. However, below blocking temperature that is at 30K hysteresis can be clearly seen in the M-H curve indicating that the nanoparticles in the ferrofluid exhibit ferrimagnetic nature [12]. The coercivity at 30K is found to be 393 Oe with a specific magnetization of 0.116emu/g which is higher than the value of 0.102emu/g at 300K.

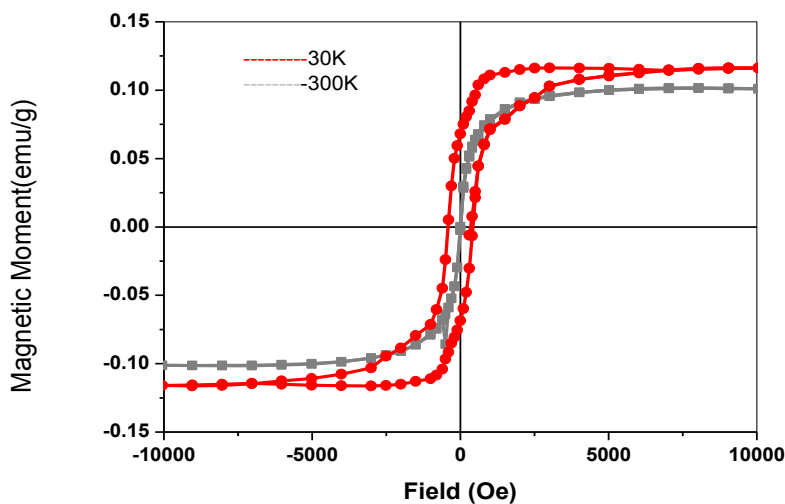


**Figure 4:** Magnetization curve of water based ferrofluid (30K and 300K).

### 3.4 Raman Characterization:

The Raman spectra of ferrofluids with varying carrier fluid viscosity are shown in Figure 5.

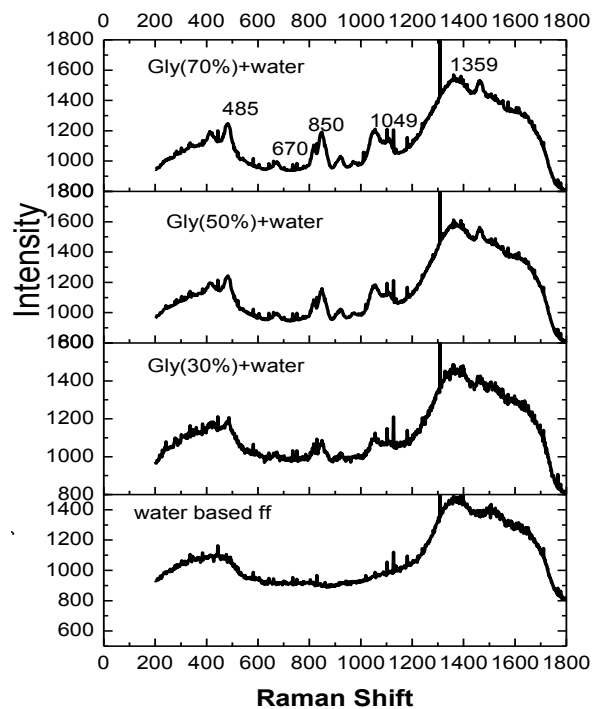


**Figure 5:** Raman spectra of ferrofluid samples. Prominent peaks are clearly seen for the ferrofluid with the highest carrier fluid viscosity. The peaks appear with lower intensities for the other ferrofluids, intensity decreasing with carrier fluid viscosity.

The prominent peaks of the spectra for the ferrofluid with highest carrier fluid viscosity are at 485, 670, 850, 1049 and 1359  $\text{cm}^{-1}$ . From the experimental results, it can be seen that as the glycerol concentration increases, the peak intensity also increases. The spectra reveal peaks of magnetite as well as maghemite due to partial oxidation [13].

### 3.5 Optical tweezer based study:

For optical tweezer based studies, a dilute ferrofluid using 1ml of wet precipitate in 50ml of carrier liquid is prepared. The principle behind optical tweezing is the suspension and subsequent trapping of micrometre sized dielectric particles by a strongly focussed laser beam and recording and analysis of the constrained motion of the particle in the trap, which will be Brownian like except for large fluctuations [14]. The deviation from pure Brownian particle like behaviour is an indicator of the trap strength. In the present work, two types of microparticles, polystyrene beads with a diameter of  $3\mu\text{m}$  and silica beads with a diameter of  $1\mu\text{m}$  are used. The trapping of these microparticles have been carried out in pure water and water-glycerol in a 70:30 admixture and the corresponding ferrofluids.

The power spectrum  $S_x(f)$  of the motion of a particle in an optical trap, where  $f$  is the frequency is given by a modified Lorentzian described by the equation

$$S_x(f) = \frac{k_B T}{\gamma \pi^2 (f_c^2 + f^2)} \tag{6}$$

Here  $k_B$  is the Boltzmann constant,  $T$  the temperature,  $\gamma$  the viscous drag co-efficient where  $\gamma = 6\pi\eta r$ , ' $\eta$ ' being the viscosity of the surrounding medium and ' $r$ ' the radius of the trapped particle [15, 16]. The Lorentzian fit of the measured power spectrum yields the corner frequency ( $f_c$ ) which is a characteristic frequency related to the trap stiffness ( $\kappa$ ) by the equation,  $\kappa = 2\pi\gamma f_c$  [17]. The trapping force is proportional to the laser power and also depends on the refractive index contrast ( $n_c$ ). The refractive index contrast is the ratio of refractive index of the bead to the refractive index of the surrounding medium ( $n_m$ ). An ideal value of refractive index contrast is 1.2 to 1.3. The maximum gradient force above the scattering force is given by,

$$F_{max} = \frac{0.49n_m P}{c} \tag{7}$$

'P' being the laser power [18]. The refractive index of silica and polystyrene probe particles at infrared wavelength range are 1.453 and 1.577 respectively [19]. Typical power spectral plot (here silica bead with a diameter of 1  $\mu\text{m}$  in water) is shown in the Figure 6.

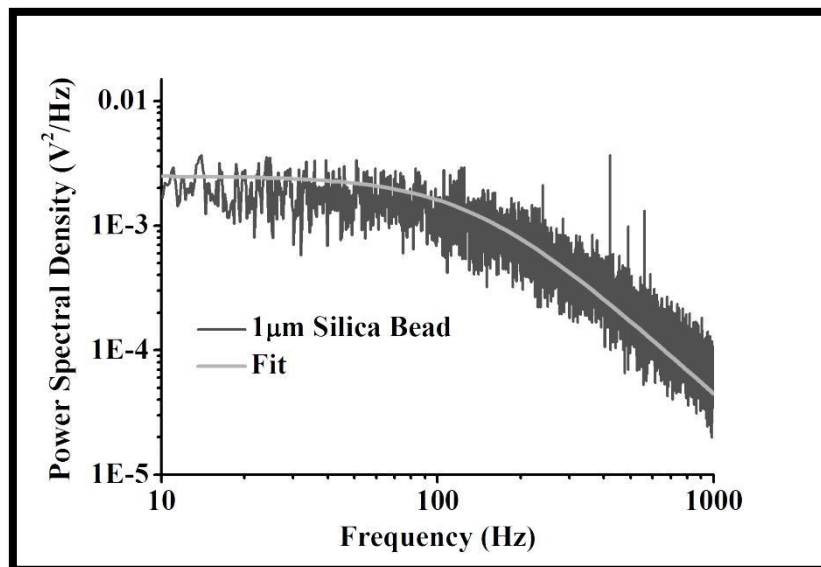


**Figure 6:** Power spectral analysis of silica bead in water.

The variation of the corner frequency with laser power at the trapping plane for both types of probe microparticles have been shown in Figure 7. We find that when the carrier fluids alone are used, an increase in carrier fluid viscosity results in a decrease in corner frequency at the same laser power. This is expected as an increase in viscosity of the surrounding medium would imply a lowering of corner frequency if trap stiffness were the same. We also find that the addition of the magnetic component results in an increase in the corner frequency when compared to the situation with the carrier fluid alone. This is irrespective of the probe used, the trapping laser power as well as the carrier fluid viscosity. We speculate that the presence of the magnetic component ought to increase the viscosity when compared to the viscosity of the carrier fluid alone, which in itself ought to have lowered the value of the corner frequency. Further we find reports of a refractive index of 1.435 for a magnetite based ferrofluid at 1557nm [20].

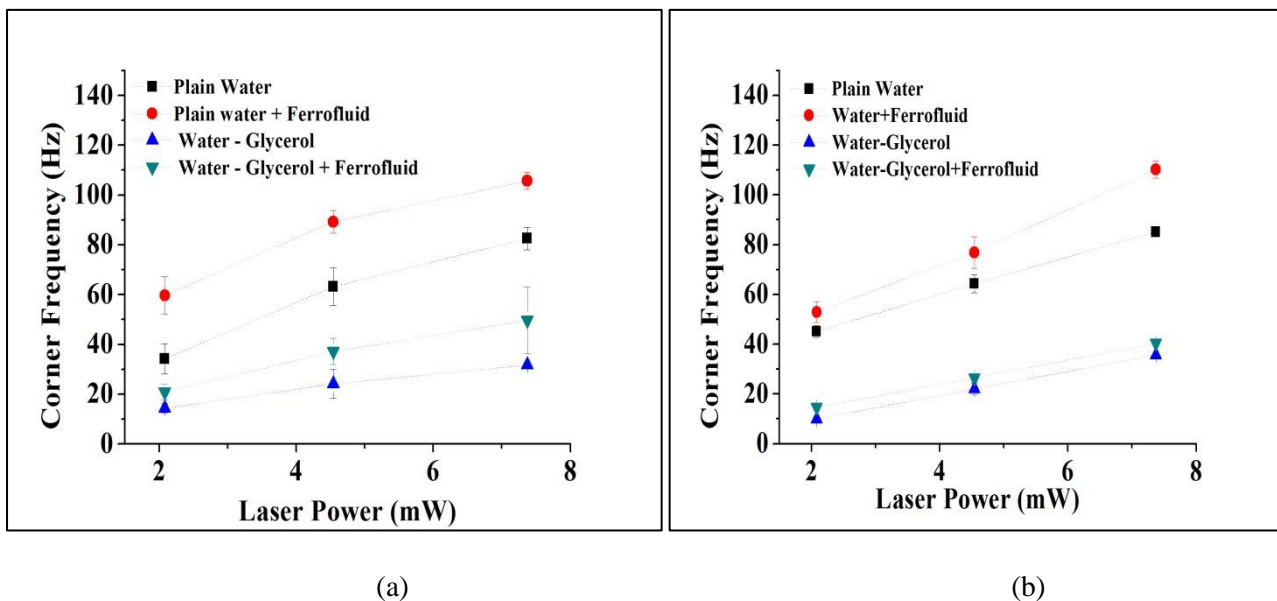


**Figure 7:** Variation of corner frequency with laser power when (a) 1µm diameter silica beads and (b) 3µm diameter polystyrene beads are trapped in various carrier fluids or ferrofluids.

Drawing from this, we speculate that the refractive index contrast is likely to lower when we use a ferrofluid, which ought to then result in a lowered trapping strength. Enhancement in the corner frequency for the ferrofluid cannot be thereby linked to either change in viscosity of the surrounding medium or to the refractive index contrast both of which would account for a lowering of the corner frequency. The increase in the corner frequency is thereby likely to be linked to the dynamics of the magnetic component in the ferrofluid. The video microscopy images of the trapped probe suggest a directed motion of the nanoparticle clusters which could lead to an additional “caging” effect of the probe particle thus registering as a heightened corner frequency. We can also speculate that the size and perhaps even shape of the magnetic clusters could play a role here.

#### 4. Conclusion

We have studied here magnetite nanoparticle based ferrofluids with varying carrier fluid viscosities. Earlier studies have shown that increase in carrier fluid viscosities lead to more stable ferrofluids. We report here using DLS studies that there is an increase in the nanoparticle cluster size as the viscosity of the carrier fluid increases. This is supported by the results from Raman spectroscopy. Analysis of the constrained Brownian motion of optically trapped non-magnetic microparticles in these ferrofluids shows that there is an increase in the corner frequency due to the presence of the magnetic component

in these materials. This is irrespective of probe size, material or trapping laser power. The viscosity and refractive index change likely due to the presence of the magnetic component cannot explain this enhancement. Taking clue from the video microscopy recordings of the trapping process we speculate that directed motion of the magnetic clusters result in an apparent enhancement of the corner frequency. As this is also likely to then depend on cluster size and shape, this technique may be a good way of characterising ferrofluids. We need to make direct measurements of the refractive index and viscosity of the ferrofluids in order to lend credence to our speculation. Further, studying the behaviour of optically trapped ferromagnetic microbeads in these ferrofluids could set up an alternate route to magnetically characterising them.

### Acknowledgements

The authors wish to acknowledge UGC, DST PURSE at Bangalore University and Prof. Ranjini Bandyopadhyay of Raman Research Institute- Bangalore for providing the DLS facility.

### References

- [1] Sadia M Hakim, 2012, "Synthesis and Characterization of ferrofluid from Iron and Manganese", Master Thesis
- [2] Javier A Lopez, Ferney Gonzalez, Flavio.A.Bonilla, Gustavo Zamrano, and Maria.E.Gomez, 2010, "Synthesis and characterization of Fe<sub>3</sub>O<sub>4</sub> magnetic nanofluid", *Revista Latinoamericana de Metallurgia Y Materials*: **30**(1): 60-66
- [3] P.Berger, N B Adelman, Beckman K J, Campbell D.J, Ellis A B and Lisensky G C, 1999, *Journal of Chemical Education*, **76**, 943-8
- [4] Savitha S and Sarbari Bhattacharya, "Synthesis and Characterization of Magnetic Colloids", to be published
- [5] Pati S S, Mahendran V, and John Philip, 2013, "A Simple Approach to Produce Stable Ferrofluids without Surfactants and with high temperature stability", *Journal of Nanofluids*, **2**, pp 94-103
- [6] Shruthi S Iyengar, Praveen P, Rekha S, Sarbari Bhattacharya, Sharath Ananthamurthy, 2016, "Autocorrelation and relaxation time measurements on metal oxide core: dielectric shell beads in an optical trap" *Proc. SPIE, Nanophotonics VI*, 98842P
- [7] Raghu A and Sharath Ananthamurthy, 2005, "Construction of an optical tweezer for nanometer scale rheology", *PRAMANA, Indian Academy of Sciences*, **65**, No. 4, physics pp. 699–705
- [8] Maria Cristina Mascolo, Yongbing Pei, Terry A Ring, 2013, "Room Temperature Co-Precipitation Synthesis of Magnetite Nanoparticles in a Large pH Window with Different Bases", *Materials*, **6**, 5549-5567
- [9] Debasish Saha, Yogesh M Joshi and Ranjini Bandyopadhyay, 2015, "Characteristics of the secondary relaxation process in soft colloidal suspension", *EPL*, **112**
- [10] Debasish Saha, Yogesh M Joshi and Ranjini Bandyopadhyay, 2015, *ACS Langmuir*, **31**, 3012-3020.
- [11] MihaMarolt, 2014, *superparamagnetic materials*, seminar content
- [12] Gamarra L F, Pontuschka W M, Mamani J B, Cornejo D R, Oliveira T R, Vieira E D, Costa-Filho A J and E aro Jr, 2009, *Journal of Physics: Condensed matter*, 115104 (6pp)
- [13] Panta P C and Bergmann C P, 2015, "Raman spectroscopy of Iron oxide nanoparticles (Fe<sub>3</sub>O<sub>4</sub>)", *International conference Material science and Engineering*.
- [14] Kathy Camenzind, 2013, Quantifying Trapping Forces in a Simplified Optical Tweezers Setup", Master Thesis
- [15] Frederick Gittes and Christoph F Schmidt, 1998, "Signal and Noise in Micromechanical measurements", *Methods in cell biology*, **55**
- [16] Keir C Neuman and Steven M. Block, 2004, *Rev Sci Instrum*, **75**(9), 2787-2809.
- [17] Jones P H, 2012, "Optical tweezers for scanning probe Microscopy", COMPLEXITPL course, M.Sc nanotechnology.
- [18] Aleksandra Radenovic, "Advanced bioengineering methods laboratory optical trapping".
- [19] Michael A Taylor, Joachim Knittel and Warwick P Bowen, 2012, arXiv.1208.0657VI, *Physics optics*.
- [20] web.phys.ntu.edu.tw/asc/FunPhysExp/2006 lecture/1.ppt

